Applied Catalysis B: Environmental 100 (2010) 62–67

Contents lists available at ScienceDirect

Applied Catalysis B: Environmental

journal homepage: www.elsevier.com/locate/apcatb

Catalytic ozonation of toxic pollutants over magnetic cobalt and manganese co-doped γ-Fe_2O_3

Aihua Lv, Chun Hu*, Yulun Nie, Jiuhui Qu

State Key Laboratory of Environmental Aquatic Chemistry, Research Center for Eco-Environmental Sciences, Chinese Academy of Sciences, Beijing 100085, China

ARTICLE INFO

Article history:
Received 4 April 2010
Received in revised form 8 July 2010
Accepted 13 July 2010
Available online 21 July 2010

Keywords:
ATR-FTIR
Catalytic ozonation
Magnetic catalyst
Multivalence
Surface Lewis acid sites

ABSTRACT

Magnetic Co- and Co, Mn-doped γ-Fe_2O_3 (FC and FCM) were prepared by co-precipitation method and characterized by X-ray diffraction (XRD), X-ray photoelectron spectroscopy (XPS), in situ attenuated total reflection FTIR (ATR-FTIR) spectroscopy and cyclic voltammetry (CV) analyses. FCM was found to be highly effective for the mineralization of 2,4-dichlorophenoxyacetic acid and its derivatives 2,4-diclorophenol, 2,4,6-trichlorophenol in aqueous solution with ozone. The characterization studies showed that Co and Mn incorporated in γ-Fe_2O_3 existed as multivalence oxidation states, and there were more Lewis acid sites on the surface of FCM. The interaction of ozone with chemisorbed H_2O and surface hydroxyl groups generated from dissociative adsorption of H_2O on Lewis acid sites initiated the production of reactive oxygen species. Moreover, a redox process was observed in the catalytic decomposition of O_3 at the water–catalyst interface by CV analysis. The results indicated that the introduction of Mn not only increased the surface Lewis acid sites of FCM to cause more surface hydroxyl groups and chemisorbed water, but also enhanced the interfacial electron transfer, resulting in higher activity.

1. Introduction

Heterogeneous catalytic ozonation has received increasing attention in recent years because of its potentially higher effectiveness in the degradation and mineralization of refractory organic pollutants and lower negative effect on water quality [1,2]. This method has been developed to overcome the limitations of ozonation processes, such as the formation of byproducts and the selective reactions of ozone designed to enhance the production of hydroxyl radicals (•OH), known as nonselective oxidants [3,4].

Supported and unsupported metals and metal oxides are the most commonly tested catalysts for the ozonation of organic compounds in water or air [5–7]. Experimental results indicate that the removal efficiencies of pollutants are significantly enhanced in the presence of catalysts compared to ozone alone. Despite these promising studies, one obstacle to its practical application is the separation of these materials from the finished water. Magnetite nanoparticles are easy to be separated from aqueous media due to their magnetic properties. Maghemite (γ-Fe_2O_3), the ferromagnetic cubic form of iron (III) oxide is technologically important, as it is being widely used for the production of magnetic materials and catalysts [8,9]. However, these magnetic catalysts have been hardly applied for the catalytic ozonation of organic pollutants in water.

The activity of the catalysts mentioned for heterogeneous ozonation is based mainly on catalytic ozone decomposition and the enhanced generation of hydroxyl radicals. The decomposition mechanism of gaseous ozone has been elucidated with in situ Raman spectroscopy and isotopic substitution [10,11]. The main redox steps were involved in the formation of superoxide or peroxide species on the surfaces of metal oxides, which suggested that transition metal oxides having easily accessible multiple oxidation states are good catalysts for ozone decomposition. In addition, the studies by our group and others [12,13] proposed that molecular ozone in aqueous solution should interact with the surface hydroxyl groups of the catalyst to initiate the formation of •OH. The amount of surface hydroxyl groups depended on the Lewis acid of the catalyst. Therefore, multiple oxidation states and surface Lewis acid sites are crucial factors for the high activity of catalyst in water.

In this present, cobalt/manganese substituted γ-Fe_2O_3 catalysts were prepared by co-precipitation method. 2,4-Dichlorophenoxyacetic acid (2,4-D) is the most widely used herbicide in the world [14]. It is poorly biodegradable and has been detected as a major pollutant in ground and surface waters. Most papers related to the treatment of chlorophenoxy herbicides in aqueous medium described the degradation of 2,4-D by advanced oxidation processes, where the mineralization of 2,4-D needed prolonging reaction time [15–17]. Therefore, 2,4-D and its derivatives 2,4-diclorophenol (2,4-DCP), together with other chlorophenols were selected to evaluate the activity and properties of the catalysts with ozone in aqueous solution. Cobalt

* Corresponding author. Tel.: +86 10 62849628; fax: +86 10 62923541.
E-mail addresses: huchun@rcees.ac.cn (C. Hu), ylnie@rcees.ac.cn (Y. Nie).

0926-3373/$ – see front matter © 2010 Elsevier B.V. All rights reserved.
doi:10.1016/j.apcatb.2010.07.011

and manganese co-substituted γ-Fe_2O_3 showed high efficiency for the degradation and mineralization of the tested toxic pollutants. This was mainly contributed to the enhanced interfacial electron transfer and the increased concentration of surface Lewis acid sites on the basis of cyclic voltammetry and in situ ATR-FTIR analyses.

2. Experimental

2.1. Materials and reagents

All reagents used in this work were analytical grade and were used without further purification. Ferric nitrate, cobalt nitrate and sodium carbonate were purchased from Beijing Chemical Reagent Company (Beijing, China). Manganese nitrate was acquired from Xilong Chemical Factory (Shantou, China). 2,4-D, 2,4-DCP and 2,4,6-trichlorophenol (2,4,6-TCP) were obtained from Yili Fine Chemicals Co., Ltd (Beijing, China). All solutions were prepared with deionized water.

2.2. Catalyst preparation

Cobalt doped γ-Fe_2O_3 (FC) was prepared by co-precipitation method. An aqueous solution containing nitrates of Fe^{3+} and Co^{2+} (molar ratio: Fe/Co = 2) was added slowly into sodium carbonate aqueous solution with continuous stirring. After aging, the precipitate was filtered and washed with deionized water, dried at 70 °C and calcined at 550 °C for 5 h in air. Cobalt and manganese co-doped γ-Fe_2O_3 (FCM) was obtained by the same method with a mixed solution of nitrates of Fe^{3+}, Co^{2+} and Mn^{2+} (molar ratio of ions: Fe/(Co + Mn) = 2, Co/Mn = 30). As a reference, iron oxide (F) was prepared by the same procedure with ferric nitrate solution.

2.3. Characterization

Powder X-ray diffraction (XRD) of the catalyst was recorded on a XDS 2000 Diffractometer (Scintag Inc., CA) with Cu Kα radiation (λ = 1.54059 Å). Magnetic measurements were conducted on a 7307 vibrating sample magnetometer (Lake Shore Cryotronics Inc., USA). The X-ray photoelectron spectroscopy (XPS) data were taken on an AXIS Ultra instrument (Kratos Analytical, UK) using monochromatic Al Kα radiation (225 W, 15 mA, 15 kV). The determination of acid groups was carried out following the method proposed by Boehm [18].

Electrochemical experiments were performed on a basic electrochemical system (Princeton Applied Research Co., U.S.A.). All experiments were done using a three-electrode cell configuration with a catalyst modified conductive glass (prepared by dip coating and drying in air at 70 °C) as the working electrode, a platinum wire as the auxiliary electrode and a saturated calomel electrode as the reference electrode.

In situ ATR-FTIR spectroscopy: To prepare an ATR sample, a desired amount of catalyst particles was added to H_2O or D_2O solution and sonicated. The manipulations were performed under nitrogen atmosphere when D_2O was employed. A short time before running the spectra, the samples were centrifuged, half of the supernatant was used as reference, the solid resuspended in the other half was used as the sample. This procedure yielded a solid concentration of 100 g L^{-1}. The ATR-FTIR spectra were recorded using a TENSOR 27 infrared spectrometer with a DLaTGS detector and a ZnSe horizontal ATR cell. Infrared spectra over the 4000–650 cm^{-1} range were obtained by averaging 32 scans with a resolution of 4 cm^{-1} at room temperature. The spectrum of the particles in suspension is the result of subtracting the spectrum of the supernatant (reference) from the spectrum of the slurry (sample). The cell remains in place throughout the running of every single-beam spectra of the empty cell, reference, and sample so that its transmittance and average angle of incidence are constant.

2.4. Procedures and analysis

Semi-batch experiments were carried out with a 1.2 L reactor. The reaction temperature was maintained at 20 °C. In a typical experiment, 1 L of 20 mg L^{-1} 2,4-D aqueous solution was introduced into the reactor. 1 g catalyst was added into this solution under magnetically stir. 30 mg L^{-1} gaseous O_3 oxygen–ozone was then bubbled into the reactor through the porous plate of the reactor bottom at a 12 L h^{-1} flow rate. Ozone gas was generated by a 3S-A5 laboratory ozonizer (Tonglin Technology, China). Samples were withdrawn at given intervals. After the residual ozone was instantly quenched with 0.1 M $Na_2S_2O_3$, each sample was filtered through a 0.45-μm cellulose acetate membrane for analysis. The gaseous ozone concentration was measured using the iodometric titration method. Concentrations of 2,4-D, 2,4-DCP and 2,4,6-TCP were measured using 1200 series HPLC (Agilent, U.S.A.) with a ZORBAX Eclipse XDB-C_{18} column (4.6 × 150 mm, 5 μm). The total organic carbon (TOC) of each solution was analyzed with a Phoenix 8000 TOC analyzer (Tekmar-Dohrmann Co., U.S.A.). The amounts of Fe^{3+}, Co^{2+} and Mn^{2+} in the supernatant were measured by inductively coupled plasma optical emission spectrometry (ICP-OES) on an OPTIMA 2000 (Perkin Elmer Co., U.S.A.) instrument.

The experiments of O_3 decomposition were carried out in sealed three-mouth 260 ml bottle. The gaseous O_3 30 mg/L (oxygen–ozone) was bubbled into the reactor to get 200 ml O_3-saturated aqueous solution (about 4 mg L^{-1}) with 60 ml, 30 mg of gaseous O_3/L oxygen–ozone mixture gas above solution. 0.2 g catalyst was added into the reactor and stirred magnetically. At given time intervals, the concentration of residual ozone in aqueous solution was monitored by UV spectrophotometer (Hitachi, Japan) using the indigo method.

3. Results and discussion

3.1. Characterization of catalysts

Fig. 1 shows the XRD patterns of different samples. The predominant crystalline phase of FC and FCM is maghemite with the reflections 2θ at 30.2, 35.6, 43.2, 57.2 and 62.7°. Weak diffraction peak was also observed at 2θ 33.2° which is related to the presence of small amounts of hematite. The results suggested that Fe, Co and Mn formed binary and ternary oxides. In contrast, the iron oxide F

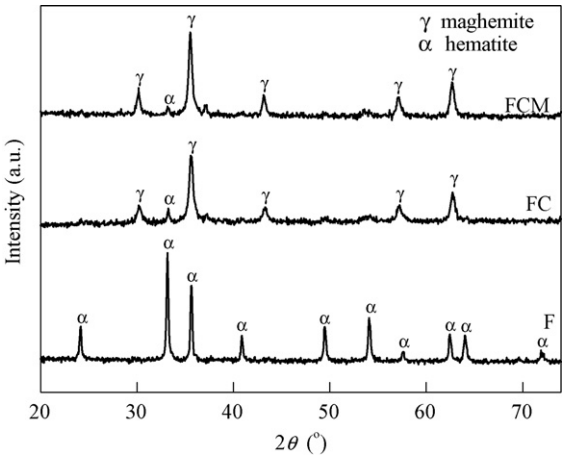

Fig. 1. XRD patterns of different catalysts.

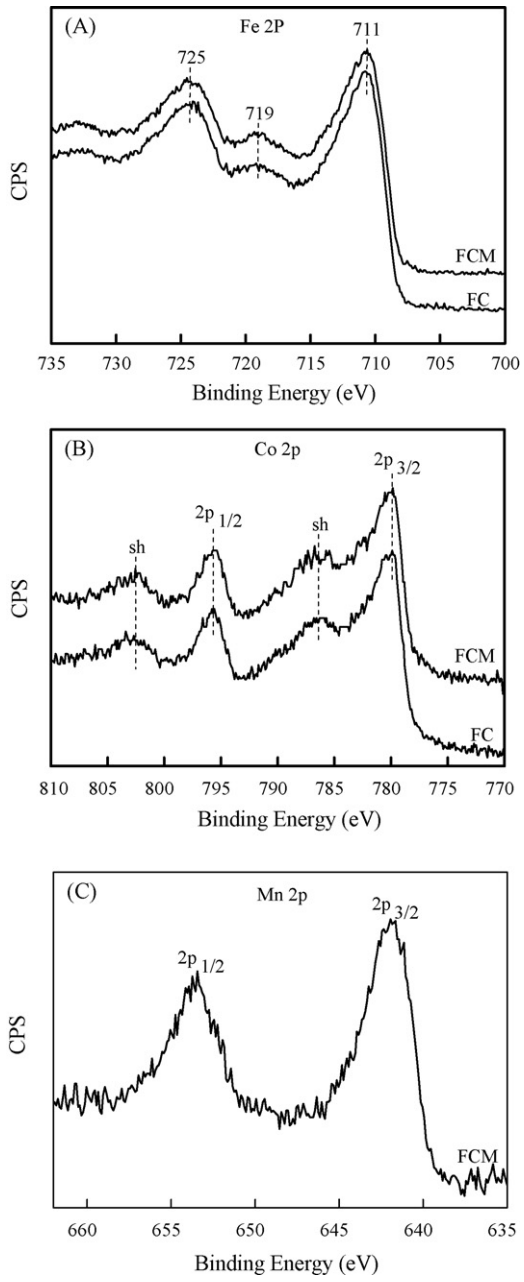

Fig. 2. XPS spectra of FC and FCM: (A) Fe 2p, (B) Co 2p, and (C) Mn 2p.

without Co and Mn is α-Fe_2O_3 phase. The results indicated that the introduction of Co and Mn enhanced the formation of maghemite. Especially, the peaks intensities of maghemite increased, while that one of α-Fe_2O_3 decreased in FCM, indicating that the incorporation of Mn more suppresses the transformation from γ- to α-Fe_2O_3. Furthermore, FCM and FC were characterized by XPS to confirm the metallic state of Fe, Co and Mn. As shown in Fig. 2A, the Fe 2p binding energy values (BE) were similar for the FC and FCM samples. The peaks at 711, 719, and 725 eV represented the binding energies of Fe $2p_{3/2}$, shake-up satellite Fe $2p_{3/2}$, and Fe $2p_{1/2}$ of Fe^{3+}, respectively. FC and FCM also exhibited similar Co 2p XPS spectra (Fig. 2B). The binding energies of 780.0 and 795.8 eV were assigned to Co $2p_{3/2}$ and Co $2p_{1/2}$ transitions, respectively. The peaks exhibited a shoulder at their high-energy side, which has to be traced back to a shake-up process. Such signals could only be observed with Co(II) compounds in the high spin state. The diamagnetic low-spin Co^{3+} ion did not show shake-up structures [19]. On the other hand, since

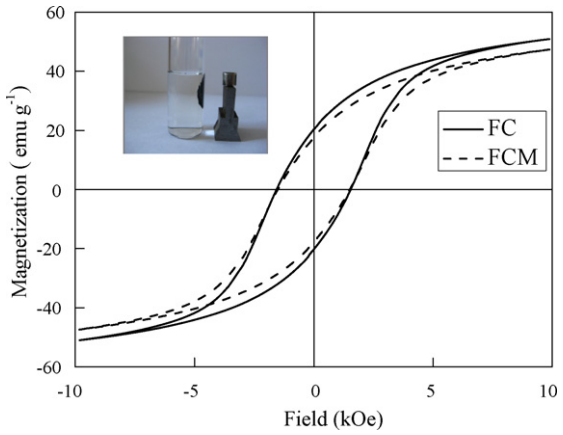

Fig. 3. Room-temperature magnetization loops of FC and FCM. The insert shows the separation of FCM from water by magnetic field.

the Co $2p_{1/2}$ signal exhibits a large difference between Co(II) and Co(III) species [20], it has been used for data evaluation although it is less intense than Co $2p_{3/2}$. The standard BE of Co $2p_{1/2}$ corresponding to CoO and Co_2O_3 respectively are 796.6 and 794.8 eV [21], while the Co $2p_{1/2}$ BE of FC and FCM is 795.8 eV. Therefore, both Co^{2+} and Co^{3+} species exist in FC and FCM. The variation of XPS binding energies of Mn 2p from Mn^{2+} to Mn^{4+} is too small (less than ~1.0 eV) to precisely evaluate the Mn valence. The Mn $2p_{3/2}$ BE value is 641.9 eV for FCM, which is attributed to $Mn^{2+/3+/4+}$ oxidation states [22,23].

3.2. Magnetic measurement and magnetic separation

Fig. 3 presents the magnetization curves of FC and FCM at room temperature up to a field of 10 kOe. The conspicuous hysteresis loops were observed, indicating that FC and FCM possess relatively harder ferromagnetic behavior. The saturation magnetization (Ms) value of FC decreased a little with Mn doping. The Ms value of FCM is 47.4 emu g^{-1} which is a little lower than 50.9 emu g^{-1} for FC. The samples could be drawn to the sidewall from the solution by applying a magnet besides the vial (Fig. 3, inset).

3.3. Surface properties

The surface of metal oxides in aqueous solution is hydroxylated due to dissociative chemisorption of water molecules, which occurs at the lattice metal ion site acting as a Lewis acid [24]. The amount and the properties of the hydroxyls depend on the metal oxide. Therefore, the surface Lewis acid concentrations of FC and FCM in water were determined by titration method. The density of acid groups of FCM was 541 μmol g^{-1}, while that of FC was 250 μmol g^{-1}. The addition of Mn increased the concentration of the surface unsaturated metal cations to enhance the surface acid properties of FC. Furthermore, in situ ATR-FTIR experiments were carried out in the D_2O solvent with N_2 atmosphere to investigate the interaction of the surface Lewis acid sites of the catalysts with water molecules. As shown in Fig. 4, the stretching vibration of the hydrogen-bonded MeO-D was 2547 cm^{-1}, while those ones of the hydrogen-bonded D_2O were 2324 and 1207 cm^{-1} [25]. The peaks intensities of FCM were stronger than those ones of FC, indicating that the more surface Lewis acid sites result in the more chemisorbed water.

3.4. Catalytic ozonation of pollutants

The catalytic activity of different catalysts was evaluated by the mineralization of 2,4-D with ozone at an initial pH 6. 2,4-D

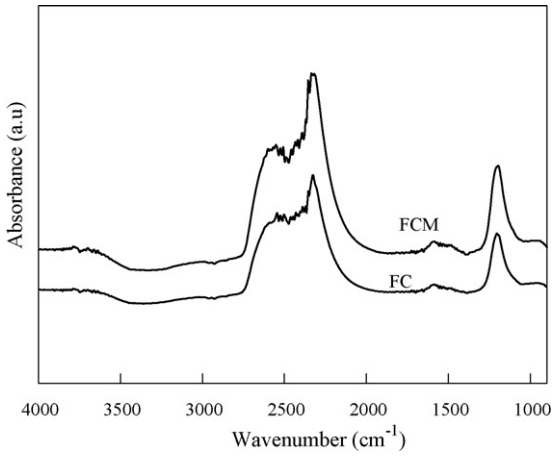

Fig. 4. ATR-FTIR spectra of FC and FCM suspended in D_2O.

had hardly any adsorption on FC and FCM under the experimental conditions, indicating that the degradation of 2,4-D occurred predominantly in solution phase. As shown in Fig. 5, only 32% of the TOC is removed at 20 min reaction with ozone alone, whereas about 64%, 34% of TOC were removed in FC and F suspension respectively at the same time. In contrast, about 93% of TOC was removed in FCM suspension under otherwise identical conditions. In 40 min, the highest released ions were Fe^{3+} 0.112 mg L^{-1} and Co^{2+} 0.134 mg L^{-1} from FC; Fe^{3+} 0.144 mg L^{-1}, Co^{2+} 0.291 mg L^{-1} and Mn^{2+} 0.039 mg L^{-1} from FCM. About 39% and 56% of TOC were removed within 20 min by their homogeneous catalytic ozonation. However, the catalytic activity of the ions in FCM suspension was much lower than FCM. The catalytic contribution of released ions was not predominant in the reaction system. The catalytic contribution of released ions was not predominant in the reaction system. The reactivity of FC markedly was enhanced by the addition of Mn due to the enhanced surface Lewis acid sites. Since the highest released ions (Fe^{3+}, Co^{2+} and Mn^{2+}) were only 0.04% of the catalyst amount, and the activity of FCM did not markedly decrease after three successive cycles of degradation testing, the results indicated that FCM was an effective and stable catalyst for catalytic ozonation.

In addition, 2,4-DCP and 2,4,6-TCP were completely degraded within 3 min, while more than 95% of TOC removal occurred within 20 min in FCM suspensions (Fig. 6).

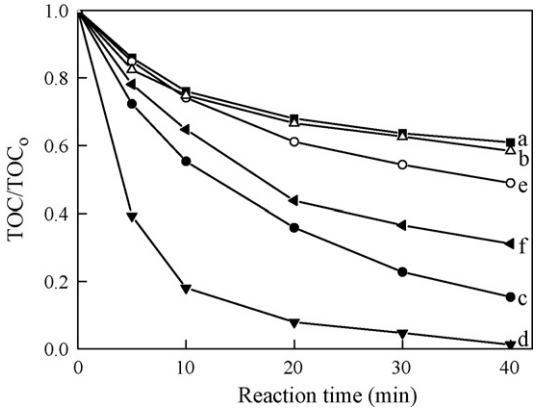

Fig. 5. Removal of TOC during the degradation of 2,4-D in aqueous dispersions of various catalysts with ozone: (a) O_3, (b) F, (c) FC, (d) FCM, (e) Fe^{3+} (0.112 mg L^{-1}) and Co^{2+} (0.134 mg L^{-1}) from FC, (f) Fe^{3+} (0.144 mg L^{-1}), Co^{2+} (0.291 mg L^{-1}) and Mn^{2+} (0.039 mg L^{-1}) from FCM (pH 6, 2,4-D: 20 mg L^{-1}, catalyst: 1 g L^{-1}, gaseous ozone concentration: 30 mg L^{-1}).

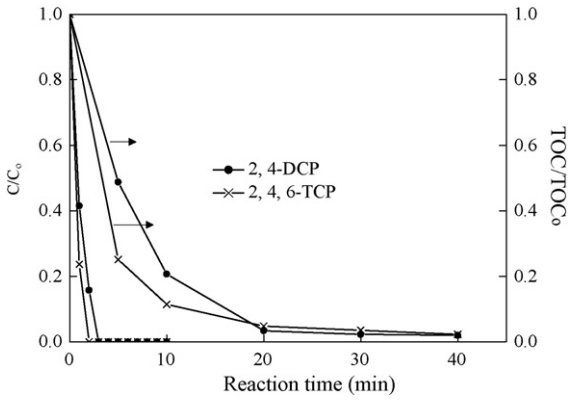

Fig. 6. Catalytic ozonation of 2,4-DCP and 2,4,6-TCP in FCM suspension (pH 6, substrate: 20 mg L^{-1}, FCM: 1 g L^{-1}, gaseous ozone concentration: 30 mg L^{-1}).

3.5. Catalytic ozonation mechanism of magnetic FCM

Tert-butyl alcohol (TBA) is a strong radical scavenger that has a reaction rate constant of 6×10^8 M^{-1} s^{-1} with hydroxyl radicals [3] and only 3×10^{-3} M^{-1} s^{-1} with ozone [26]. It can terminate radical chain reactions by generating inert intermediates. Thus, TBA was adopted as the indicator for a radical-type reaction. As shown in Fig. 7, for the removal of 2,4-D, both ozone alone and FCM with ozone exhibited similar reaction efficiency, which has been observed in the previous work [27]. However, for the mineralization of 2,4-D, the oxidation performance of ozone was not enough, while the catalytic ozonation using FCM showed significantly enhanced activity. Similarly, the degradation of 2,4-D was depressed with the addition of *t*-butyl alcohol under both conditions. These results indicated that •OH radicals were the main active species for the oxidation of 2,4-D in both ozone alone and FCM with ozone. On the other hand, in ozone alone system, the active species might depend on different pollutants. It has been verified that the •OH radicals were not main in the degradation of ibuprofen with ozone alone [12].

Meanwhile, a series of ozone decomposition experiments were carried out in the presence of the studied catalysts. Clearly, the ozone decomposition was enhanced by different catalysts in Fig. 8, while FCM showed slightly higher removal rate compared to FC. Since the decomposition of O_3 is a chain reaction, the reactive species generated from the decomposition of O_3 were not consumed due to the absence of pollutant in the experiments, leading the rate difference for the O_3 decomposition smaller. The same

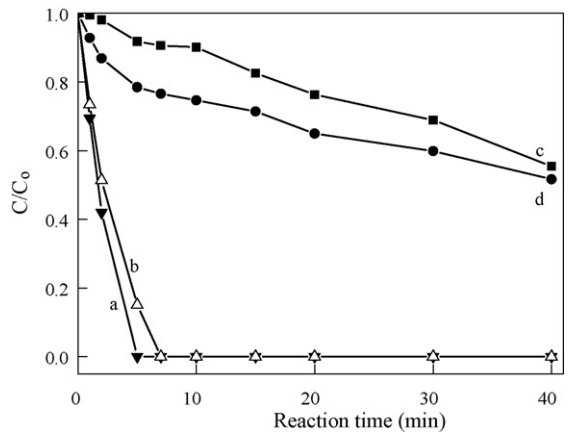

Fig. 7. Effect of tert-butanol (10 mM) on the degradation of 2,4-D at pH 6: (a) O_3, (b) O_3/FCM, (c) O_3 + tert-butanol, (d) O_3/FCM + tert-butanol (2,4-D: 20 mg L^{-1}, catalyst: 1 g L^{-1}, gaseous ozone concentration: 30 mg L^{-1}).

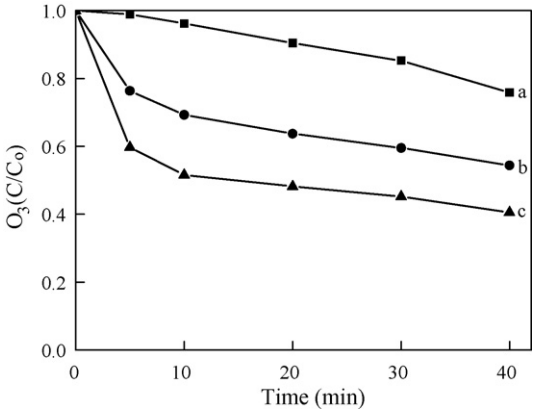

Fig. 8. Decomposition of ozone in aqueous dispersions of various catalysts: (a) without catalyst, (b) FC, and (c) FCM.

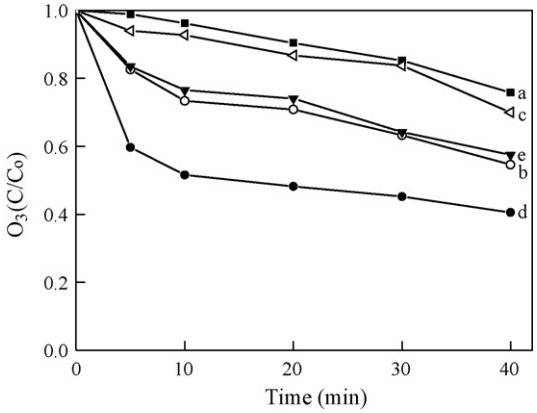

Fig. 10. Effect of phosphate on decomposition of ozone aqueous solution under different conditions: (a) O_3 alone, (b) 5 mM phosphate, (c) 1 M phosphate, (d) FCM, and (e) FCM + 5 mM phosphate.

phenomenon was also observed by other researchers [28,29]. They thought that the decomposition of O_3 was two stages, the first one is the faster decomposition of O_3, fitting a first-order kinetic expression, while the second one also fits a first-order kinetic expression, its rate is lower.

Bulanin et al. [30] suggested that in gaseous phase, ozone dissociates after adsorption on strong Lewis sites yielding a surface oxygen atom, whereas on weaker sites, ozone molecules coordinate via one of the terminal oxygen atoms. In aqueous phase, it could not be confirmed whether the same process occurs due to H_2O, OH^- and other hard Lewis bases commonly present in water. However, it has been verified that the more surface Lewis acid sites result in more surface hydroxyl groups and chemisorbed water, causing more reactivity. In order to verify the role of the surface properties, phosphate was used to investigate the mechanism of the catalytic ozonation due to its strong bonding with the Lewis acid sites of the catalyst.

Firstly, the effects of phosphate on the catalytic ozonation of 2,4-D and catalytic decomposition of O_3 were carried out in FCM suspension. Obviously, the catalytic activity of FCM was greatly depressed in the presence of 5 mM phosphate while the efficiency of ozone alone was significant enhanced from 39% to 64% TOC removal at 40 min reaction with the addition of 5 mM phosphate (Fig. 9). Correspondingly, as shown in Fig. 10, the decomposition of O_3 was significantly enhanced in 5 mM phosphate aqueous solution. The decomposition of O_3 belonged to the chain reaction, producing free radicals, which could be scavenged by the radical scavenger and organics, thus accelerating the decomposition of O_3 [31,32]. The observation is different from those reported [31]. However, with the phosphate concentration increasing, the decomposition rate of O_3 decreased. In these experiments with different phosphate concentration, the solution pH was kept at pH 7 by adjusting the addition ratio of Na_2HPO_4 and NaH_2PO_4. The formation of phosphate in water mainly depended on solution pH. Therefore, the characters of phosphates in these experiments were same although their concentrations were different. For the O_3 decomposition experiment in pure water, the initial pH 7 of solution was adjusted by 0.1 M NaOH solution, and the solution pH was about 7.5 after the reaction finished, so the pH changes favored the decomposition of O_3. The interaction of phosphate with ozone still needs to be investigated further in detail in another work. Nevertheless, the catalytic decomposition of O_3 was greatly depressed by 5 mM phosphate, and its rate was similar to that one in ozone alone with phosphate. This result indicated that the catalyst hardly played any role in the decomposition of O_3 in the presence of phosphate. Furthermore, the changes of FCM surface properties were observed by in situ ART-FTIR with the addition of phosphate (Fig. 11). The peaks at 3470 and 3130 cm^{-1} in FCM suspension are assigned to hydrogen-bonded MeO-H and H_2O. However, the signals significantly decrease in the presence of phosphate, and two new peaks appear at 1011 and 1127 cm^{-1}, belonging to phosphate vibrations [25]. Phosphate holds the surface Lewis acid sites on the catalyst preventing chemisorption of water, leading to the lower catalytic activity. The results indicate that the surface hydroxyls

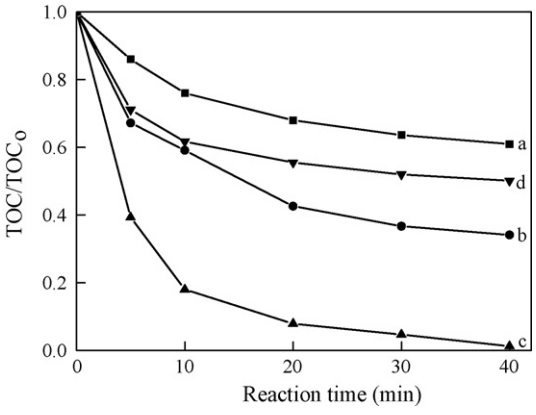

Fig. 9. Effect of phosphate on the degradation of 2,4-D in different ozone aqueous solution: (a) O_3 alone, (b) 5 mM phosphate, (c) FCM, (d) FCM + 5 mM phosphate (2,4-D: 20 mg L^{-1}, catalyst: 1 g L^{-1}, gaseous ozone concentration: 30 mg L^{-1}).

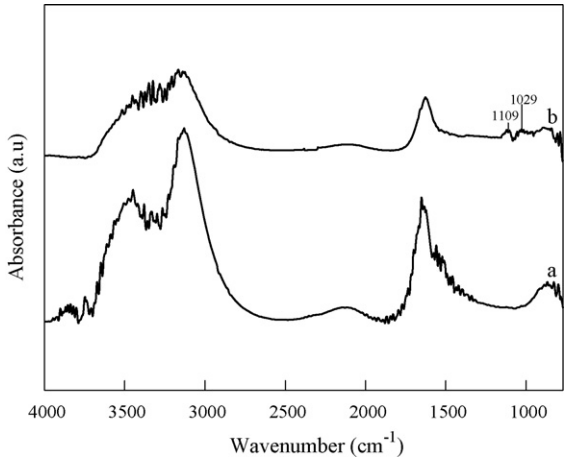

Fig. 11. ATR-FTIR spectra of FCM suspended in water: (a) without phosphate, (b) with 10 mM phosphate.

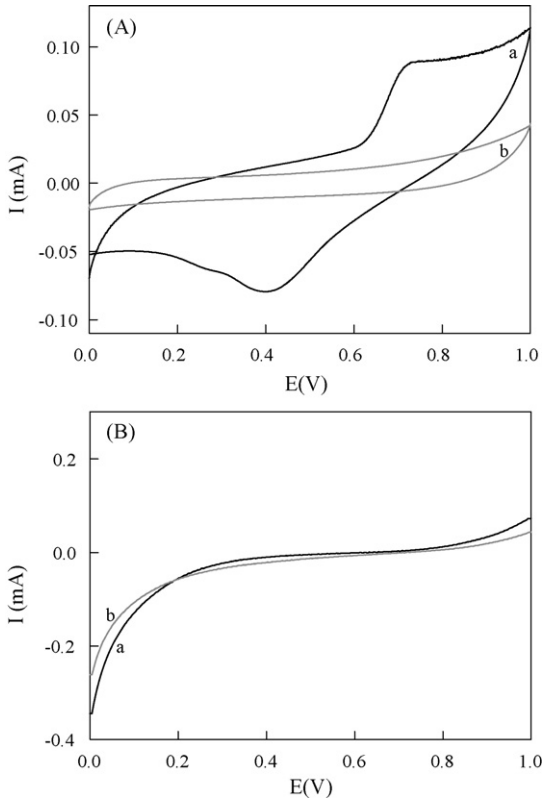

Fig. 12. Cyclic voltammetry scans with FC (a) and FCM (b) electrodes in a 0.1 M sodium sulfate aqueous solutions without (A) and with (B) O_3.

and chemisorbed water are active sites for the interaction of O_3 with the catalyst, while the Lewis acid sites are reactive center for catalytic ozonation in aqueous phase.

In order to observe the electron transfer process at water–catalyst interface, the cyclic voltammetry behaviors of FC and FCM film electrodes were investigated in a 0.1 M Na_2SO_4 solution at air or ozone atmosphere. As shown in Fig. 12, no obvious redox peaks were observed at the FC electrodes. However, the FCM film electrode gave a couple of stable and well-defined redox peaks at 0.40 V and 0.72 V, which was possibly contributed to the cycle of Mn^{2+}/Mn^{3+} or Mn^{4+} in FCM. The results indicated that the addition of Mn enhanced the electron transfer process. With the addition of ozone, both FC and FCM did not exhibit any current signal, indicating that a redox process occurred at the surface of the catalyst during the catalytic decomposition of O_3, which was agreed with several reports [4,33]. These results reveal that the introduction of Mn not only increases the surface Lewis acid sites but also enhances the interfacial electron transfer, resulting in a higher catalytic activity.

4. Conclusions

Magnetic magnetite FC and FCM composites were prepared by co-precipitation method, which combined the advantages of high dispersion and reactivity with easy magnetic separation. FCM showed higher efficiency for the mineralization of 2,4-D, 2,4-DCP and 2,4,6-TCP aqueous solution with ozone. Dissociative chemisorptions of D_2O occurred at the surface Lewis acid sites of the catalyst, and interacted with ozone to initiate the generation of reactive oxygen species. Moreover, a redox process was observed in the catalytic decomposition of O_3 at the water–catalyst interface by CV analysis. The introduction of Mn not only increased the surface Lewis acid sites of FCM to cause more surface hydroxyl groups and chemisorbed water, but also enhanced the interfacial electron transfer, resulting in higher activity.

Acknowledgments

This work was supported by the National Natural Science Foundation of China (No. 20977104, 50908223, 50921064) and the Chinese Academy of Sciences (kzcx1-yw-06-02,08Z01ESPCR) and the 973 project (2010CB933600).

References

[1] B. Kasprzyk-Hordern, M. Ziółek, J. Nawrocki, Appl. Catal. B: Environ. 46 (2003) 639–669.
[2] F.J. Beltrán, F.J. Rivas, R. Montero-de-Espinosa, Ind. Eng. Chem. Res. 42 (2003) 3218–3224.
[3] C.P. Huang, C. Dong, Z. Tang, Waste Manage. 13 (1993) 361–377.
[4] B. Legube, N.K.V. Leitner, Catal. Today 53 (1999) 61–72.
[5] R. Gracia, S. Cortes, J. Sarasa, P. Ormad, J.L. Ovelleiro, Water Res. 34 (2000) 1525–1532.
[6] F. Delanoë, B. Acedo, N.K.V. Leitner, B. Legube, Appl. Catal. B: Environ. 29 (2001) 315–325.
[7] F.J. Beltrán, F.J. Rivas, R. Montero-de-Espinosa, Appl. Catal. B: Environ. 47 (2004) 101–109.
[8] N.K. Prasad, K. Rathinasamy, D. Panda, D. Bahadur, J. Mater. Chem. 17 (2007) 5042–5051.
[9] F. Shi, M.K. Tse, M.-M. Pohl, J. Radnik, A. Brückner, S. Zhang, M. Beller, J. Mol. Catal. A: Chem. 292 (2008) 28–35.
[10] W. Li, G.V. Gibbs, S.T. Oyama, J. Am. Chem. Soc. 120 (1998) 9041–9046.
[11] W. Li, G.V. Gibbs, S.T. Oyama, J. Am. Chem. Soc. 120 (1998) 9047–9052.
[12] L. Yang, C. Hu, Y. Nie, J. Qu, Environ. Sci. Technol. 43 (2009) 2525–2529.
[13] L. Zhao, Z. Sun, J. Ma, Environ. Sci. Technol. 43 (2009) 4157–4163.
[14] E. Brillas, J.C. Calpe, P.-L. Cabot, Appl. Catal. B: Environ. 46 (2003) 381–391.
[15] J.J. Pignatello, Environ. Sci. Technol. 26 (1992) 944–951.
[16] R.G. Zepp, B.C. Faust, J. Hoigne, Environ. Sci. Technol. 26 (1992) 313–319.
[17] M. Trillas, J. Peral, X. Domčnech, Appl. Catal. B: Environ. 5 (1995) 377–387.
[18] H.P. Boehm, Adv. Catal. 16 (1966) 179–274.
[19] M. Voß, D. Borgmann, G. Wedler, J. Catal. 212 (2002) 10–21.
[20] A. Foelske, H.-H. Strehblow, Surf. Interface Anal. 29 (2000) 548–555.
[21] I. Milošev, H.-H. Strehblow, Electrochim. Acta 48 (2003) 2767–2774.
[22] G. Qi, R.T. Yang, J. Phys. Chem. B 108 (2004) 15738–15747.
[23] H. Chen, A. Sayari, A. Adnot, F. Larachi, Appl. Catal. B: Environ. 32 (2001) 195–204.
[24] H. Tamura, A. Tanaka, K. Mita, R. Furuichi, J. Colloid Interface Sci. 209 (1999) 225–231.
[25] M.I. Tejedor-Tejedor, M.A. Anderson, Langmuir 2 (1986) 203–210.
[26] R. Andreozzi, V. Caprio, A. Insola, R. Marotta, Catal. Today 53 (1999) 51–59.
[27] S. Xing, C. Hu, J. Qu, H. He, M. Yang, Environ. Sci. Technol. 42 (2008) 3363–3368.
[28] W.-J. Huang, G.-C. Fang, C.-C. Wang, Colloids Surf. A: Physicochem. Eng. Aspects 260 (2005) 45–51.
[29] H. Valdés, F.A. Murillo, J.A. Manoli, C.A. Zaror, J. Hazard. Mater. 153 (2008) 1036–1042.
[30] K.M. Bulanin, J.C. Lavalley, A.A. Tsyganenko, Colloids Surf. A: Physicochem. 101 (1995) 153–158.
[31] J. Staehelln, J. Hoigné, Environ. Sci. Technol. 16 (1982) 676–681.
[32] H. Taube, W.C. Bray, J. Am. Chem. Soc. 62 (1940) 3357–3373.
[33] P.C.C. Faria, J.J.M. Órfão, M.F.R. Pereira, Catal. Commun. 9 (2008) 2121–2126.